Climate Dynamics (1997) 13 : 757–767

Climate Dynamics

Simulation of the influence of solar radiation variations on the global climate with an ocean-atmosphere general circulation model

U. Cubasch[1], R. Voss[1], G. C. Hegerl[2], J. Waszkewitz[1], T. J. Crowley[3]

[1] Deutsches Klimarechenzentrum GmbH, Bundesstr. 55, D-20146 Hamburg, Germany
[2] Max-Planck-Institut für Meteorologie, Bundesstr. 55, D-20146 Hamburg, Germany
[3] Dept. of Oceanography, Texas A&M University, College Station TX 77843, USA

Received: 14 October 1996 / Accepted: 9 May 1997

Abstract. Two simulations with a global coupled ocean-atmosphere circulation model have been carried out to study the potential impact of solar variability on climate. The Hoyt and Schatten estimate of solar variability from 1700 to 1992 has been used to force the model. Results indicate that the near-surface temperature simulated by the model is dominated by the long periodic solar fluctuations (Gleissberg cycle), with global mean temperatures varying by about 0.5 K. Further results indicate that solar variability and an increase in greenhouse gases both induce to a first approximation a comparable pattern of surface temperature change, i.e., an increase of the land-sea contrast. However, the solar-induced warming pattern in annual means and summer is more centered over the subtropics, compared to a more uniform warming associated with the increase in greenhouse gases. The observed temperature rise over the most recent 30 and 100 years is larger than the trend in the solar forcing simulation during the same period, indicating a strong likelihood that, if the model forcing and response is realistic, other factors have contributed to the observed warming. Since the pattern of the recent observed warming agrees better with the greenhouse warming pattern than with the solar variability response, it is likely that one of these factors is the increase of the atmospheric greenhouse gas concentration.

1 Introduction

The potential role of solar variability as an agent for climate change has long been discussed. Although there is an 11-year cycle in solar variability that is associated with only about a 0.1% change in solar irradiance, longer term variations in the Sun could conceivably cause larger climate variations. Such natural changes could complicate the identification of a human-induced climate signal in the observed record.

In the last few years evidence has accumulated for some level of significant impact of solar variability on climate on decadal-centennial time scales (e.g., Wigley and Kelly 1990; Friis-Christensen and Lassen 1991; Reid 1991; Hoyt and Schatten 1993; Lean et al. 1995; Lean 1997; Crowley and Kim 1993, 1996). Research interest has also been heightened by new estimates from solar models of potential changes in solar radiation of 0.24–0.30% on centennial time scales (Hoyt and Schatten 1993; Lean et al. 1995; Lean 1997). This value is valid for the top-of-the-atmosphere. Taking geometry into consideration (reduction to 1/4), and assuming a global albedo of 0.3, only about 17.5%, i.e., 0.5 to 0.75 W/m^2 of the solar radiation changes will be absorbed by the surface/troposphere system. This number should be compared to the best available estimate of the radiative forcing by the increase of anthropogenic greenhouse gases from pre-industrial (1880) to present-day concentrations (1992) of 2.4 W/m^2 (IPCC 1996). Calculations with energy balance models (Reid 1991; Crowley and Kim 1996) and an atmospheric general circulation model (AGCM, Rind and Overpeck 1993) suggest that such relatively small changes could still cause surface temperature changes on the order of several tenths of a degree centigrade.

Although the AGCM study of Rind and Overpeck (1993) examined the surface temperature response to a reduction of the solar radiance during the Maunder Minimum (1650–1710), to date no one has published a study illustrating the time dependent response to solar forcing in a coupled ocean-atmosphere GCM (O-AGCM). Due to the different response times of land and sea, and the extra degrees of freedom with a varying ocean, the time varying response to solar variability could be significantly different from the mean response.

In this study we examine the potential effect of solar variability on climate by forcing the O-AGCM ECHAM3/LSG with the Hoyt and Schatten (1993) solar index. Specific objectives involve determining the potential magnitude and spatial and temporal patterns of temperature change and evaluating the implication of results for interpretation of the twentieth century warming trend.

Correspondence to: U. Cubasch
E-mail: cubasch@dkrz.de

Note that due to the high uncertainty associated with the estimate of solar radiation changes, we emphasize that we are evaluating the response to the potential change in forcing. By choosing an estimate of solar variability that might be considered generous by some, we are hoping to enhance the signal-to-noise ratio. Some additional feedback mechanisms, such as UV-induced changes in stratospheric chemistry, might amplify the effect of solar variability even further and cause an additional temperature response (see Ramaswamy et al. 1996).

2 Model and experiment design

All simulations were carried out using a new version (ECHAM3/LSG; see Voss et al. 1997) of the Hamburg O-AGCM (Cubasch et al. 1992; Maier-Reimer et al. 1993; Roeckner et al. 1992), with a resolution of T21 and with 19 levels in the atmosphere, and 11 levels in the ocean. The model includes the diurnal cycle and comprehensive physical parametrizations, such as cloud liquid water as a prognostic variable (DKRZ 1993). The model has been used for a number of climate and climate change experiments (Cubasch et al. 1995; Hasselmann et al. 1996; Hegerl et al. 1996, 1997), whose results have been included in the most recent IPCC report (IPCC 1996). The model's sensitivity to a doubling of CO_2 is estimated from a 500 y simulation to be 2.5 K (Voss et al. 1996).

The experiments discussed in the present study consist of three simulations:

a. A control simulation (CTL) with fixed solar radiance of 1365 W/m^2, which at the time of this analysis had been run for more than 700 y. During the first 160 y the control simulation shows an increase of the globally averaged near-surface temperature of 0.5 K, which is mainly caused by adjustment processes of the coupled model at the Antarctic sea-ice edge. This drift is likely to be caused by imbalances of the fluxes exchanged between ocean and atmosphere (von Storch et al. 1996). In order to reduce the impact of this drift, the climate change has been calculated by subtracting the respective year of the control simulation from each year of the climate change simulation ("definition 2" of Cubasch et al. 1994). Since anomalies computed with this technique show artificially enhanced variability, a different technique to remove the trend has been used for the spectral analysis (see Sect. 3). In that case we have fitted an exponential function to the time series of the first empirical orthogonal function (EOF) (North 1984; Preisendorfer 1988) and subtracted the fitted time evolution of the first EOF from the simulation. This method corrects for most of the drift in the control run. Sensitivity tests using this technique rather than definition 2 for other work in this study did not alter the basic conclusions of the study.

b. Two solar variability experiments which started in the year 1700 and were integrated to 1992. The changes in the solar radiance in the latter experiments have been prescribed following the estimates of Hoyt and Schatten (1993). The solar radiance has been normalized so that its average value equals the (fixed) value of the solar radiance in the control simulation. Since the solar radiance at 1700 starts with a lower than average value, a 20 year spin-up run has been carried out in which the solar radiance has gradually been reduced from the average value to the 1700 value. The two experiments were started from two different initial conditions (160 years apart) of the control simulation. Since the use of "definition 2" to calculate the climate response increases the noise by a factor of two, two experiments have been run to enable a better separation of the temperature response to solar radiation changes from that due to noise induced climate variability.

Although solar studies indicate that UV variability is proportionately greater than variability in the visible band, no attempt has been made to adjust the model forcing to changes in solar variability by wavelength. We consider such an approach justifiable at this stage of assessment of the sun-climate linkage because Lean et al. (1995) estimate that peak-to-trough changes in UV radiation in the 200–300 μm band represent only 7% of the total irradiance change. Such an amount should not greatly affect our calculation of the response of near-surface temperature, but it could affect the changes with height calculated by the model (see later).

The time series of estimated solar radiance changes (Hoyt and Schatten 1993; see Fig. 1a) is derived from five different proxy measures, mostly related to historical sunspot observations, which are considered a measure of secular changes in solar convective energy transport and thus of solar irradiance changes. The time series of estimated solar irradiance changes is clearly subject to high uncertainty imposed by the uncertainties in the proxies and additionally in the relation of these proxies to solar irradiance change. Note that there are also some differences between the estimates of solar variability by Hoyt and Schatten (1993) and one derived by Lean et al. (1995). The former is about 20% larger than the latter and timing of changes is also phase-shifted by 20 y (see further discussion in Crowley and Kim 1996).

3 Results

3.1 Global mean response

Differences in the near surface temperature response to solar forcing are illustrated in Fig. 1b. Of the fluctuations of about 5 W/m^2 (peak-to-trough) in solar irradiance, only 16% actually reaches the surface (i.e., the albedo in the model is slightly higher, 0.36, than the 0.3 assumed in the bulk estimate in the introduction). This fluctuation of the solar input causes global mean temperature changes of about 0.5 K. This response is approximately the expected value ($\sim$0.42 K) for a model with an equilibrium sensitivity of about 0.6 K/(W/m^2) once the effect of spherical geometry and albedo are accounted for (see introduction). The Little Ice Age response in the model is comparable to the estimated temperature change between 1700–1850 (0.4 K) in the Bradley and Jones (1993) time series, once that time series has been rescaled to hemispheric mean annual temperatures (see Crowley and Kim 1996).

After correcting for the differences in sensitivity between the linear EBM run of Crowley and Kim (1996) and

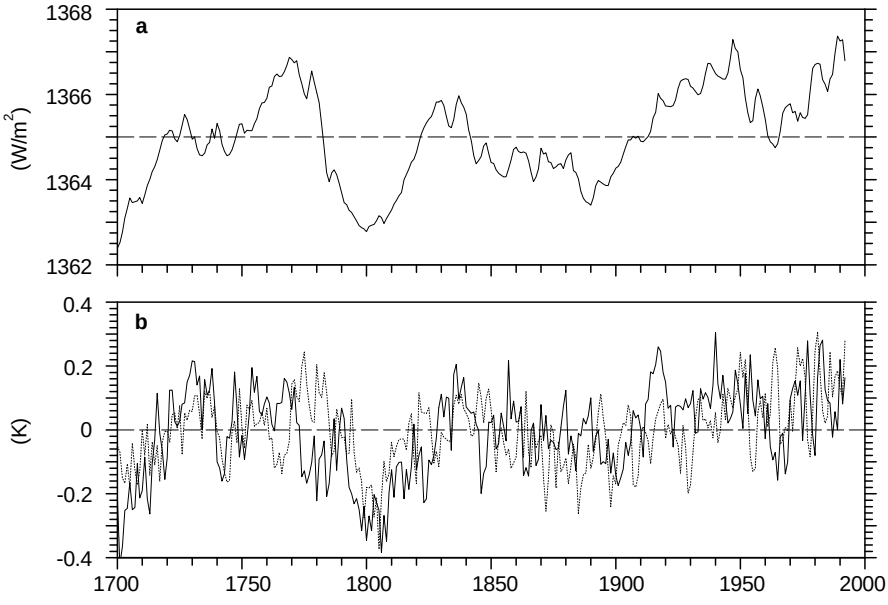

Fig. 1. **a** The solar radiance after Hoyt and Schatten (1993), normalized so that its average value is 1365 W/m^2, **b** the global mean near-surface temperature response to the solar variability for both experiments

the coupled model, the temperature reponse of the latter model is about one third larger than with the EBM. This is because the coupled model responds more to a decrease in the solar radiance (max. 0.3 K) than to an increase (max 0.2 K). This is likely due to the strong sign dependence of ice-albedo feedback, which has also been found in other simulations (Spelman and Manabe 1984; Manabe et al. 1991; Roeckner et al. 1995). Assuming no underlying long periodic variability, the simulated twentieth century warming of 0.20 ± 0.05 K (linear regression coefficient $\pm$ 95% confidence interval for trend estimate) represents less than one-third of the observed change (0.53 ± 0.09 K) over the latest 100 years (Jones and Briffa 1992). Similar results were obtained by Lean et al. (1995) and Crowley and Kim (1996). During the last 30 y the rise in the solar radiance by 2.3 W/m^2 (at the top of the atmosphere) causes the temperature to rise by about 0.16 ± 0.09 K, compared to 0.54 ± 0.13 K of the simulated global warming by greenhouse gas forcing (Hegerl et al. 1997) and 0.39 ± 0.15 K for the observations. The ± 0.15 K uncertainty in our runs represents the 95% confidence interval in the estimation of a linear trend from noisy data. The confidence intervals of the latest 30-y trends of observations and solar simulations are significantly different at the 95% level. However, they do not take the uncertainty caused by superimposed longer term natural climate fluctuations into account and thus the significance level is over-estimated. A formal signal-to-noise analysis has been performed in order to decide if the recent observations are in fact inconsistent with solar forced climate change alone at some significance level (see Sect. 3.5).

Figure 1 also shows a large quasi-cyclic response that is associated with the (88 year) Gleissberg cycle in solar forcing. The solar variability boosts the standard deviation of the global mean near surface temperature of the CTL simulation by about 60%. A spectral decomposition shows that the ECHAM3/LSG control simulation (Fig. 2) has higher variance at shorter periods (< 40 y) than an earlier version, the ECHAM1/LSG model (von Storch et al. 1996; Hegerl et al. 1996, 1997; not shown). The variance on longer time scales is lower than in the older model (Covey et al. 1996). However, the comparison is problematic since the very-low-frequency variability of the earlier model may be artificially enhanced due to a strong event or model equilibration at the beginning of the simulation (von Storch et al. 1996). The variability of ECHAM3/LSG is somewhat lower than that of the GFDL model or the Hadley Centre model, the latter showing more variability than the observations (see Covey et al. 1996; Santer et al. 1996b; Hegerl et al. 1997; Stouffer et al. in preparation).

Since the observed decadal and longer-term climate variability, and the contribution to it by forced variations, is poorly known at present it is impossible to assess which climate model exhibits the most realistic variability at these time scales. In the solar variability experiments, the model generated long-term variability with periods longer than 50 y is significantly enhanced and is now higher than in the GFDL or Hadley Centre control simulations. This response coincides with the spectral interval where the solar variability provides the largest input. This increased variance at lower frequencies improves on the model "deficiency" discussed by Barnett et al. (1996), i.e., an underestimate of long-term variability (periods longer than 30 y) in all available OAGCM simulations relative to observations.

There is little indication that the short-term model variability is enhanced, even though the prescribed solar variability has a relative maximum at frequencies of about 11 years. Nor is there any evidence for an enhanced 22-y Hale solar cycle response in the model, even though the maximum regional temperature response in the model occurs in the same region of North America (Fig. 3) where the Hale cycle was first detected at a statistically significant level in tree ring records (Mitchell et al. 1979). This muted response may be an indication that the climate

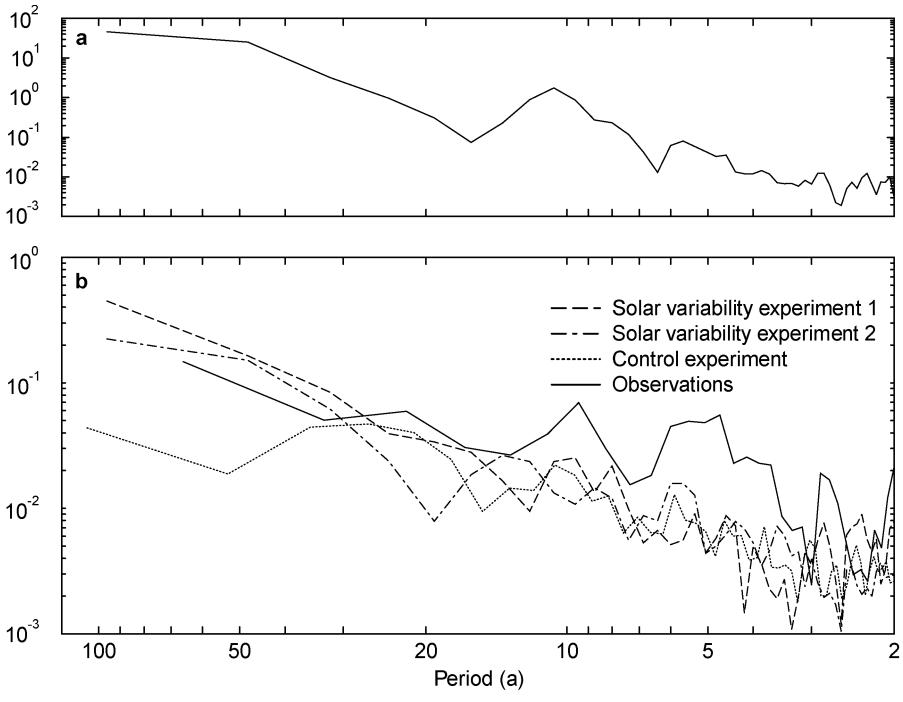

Fig. 2a,b. Spectra of **a** the solar variability time series and **b** of global mean near-surface temperature for the solar variability experiments, the control experiment and the observations. To allow comparisons, all global averages have been computed using only areas where enough observed data are available after 1949

model is not sensitive enough and that the vertical resolution and the parametrization of physical processes within the stratosphere might not be adequate to obtain realistic responses to the prescribed small radiative fluctuations on this time scale.

3.2 Regional response

We also examined the regional response to solar forcing variations. Contrary to analyses of global warming simulations (Cubasch et al. 1992), an analysis of the empirical orthogonal functions (EOF analysis, for details see North 1984; Preisendorfer 1988) did not yield a stable response pattern to changes in solar radiation, since the solar forcing is weaker than the anthropogenic forcing and thus the signal-to-noise ratio of the climate response is smaller. The spatial pattern of the first EOF was thus strongly contaminated by superimposed noise patterns. The EOF also disregards information contained in the time series of the solar forcing.

A better way to isolate a response pattern to temporally varying forcing is to compute the spatial pattern of the covariance between the solar variability and the mean temperature response of both solar forcing simulations (each relative to the instantaneous state of the control simulation) at each gridpoint (Fig. 3a). The covariance has been normalized by the variance of the forcing (yielding the near surface temperature change per W/m^2 of forcing). This can be alternatively understood as a linear regression of the solar forcing time series upon the model response.

The resultant temperature response is similar to that obtained in greenhouse-gas simulations (Santer et al. 1994; Cubasch et al. 1994). Both solar and greenhouse-gas forcing yield near surface temperature response patterns that are largely dominated by land-sea contrast (Fig. 3a, b). In the high latitudes of both hemispheres the natural variability is so large that a significant link between solar variability and temperature change could not be established based on only two simulations. Figure 3c shows the differences between the temperature response to solar forcing changes and the greenhouse-gas induced pattern (after both are normalized to the same overall variance). Differences occur on rather large spatial scales. Generally, the solar forcing seems to produce enhanced warming of the subtropical regions, especially over the eastern Pacific.

We cannot, at present, distinguish whether these differences are caused by the different nature (see Kiehl and Briegleb 1993) or time history of the forcing, or whether differences are an artifact to climate variability. Considerably more analysis (and simulations) are required to study this problem in depth. If verified, we can speculate that the pattern differences reflect the different nature of the forcing: the heating due to the increased CO_2 concentration is caused by an enhanced absorption of infrared radiation, while solar variability heats the atmosphere via an increased flux of shortwave radiation, which can only reach the ground in cloud-free regions. The link between solar variability and surface temperature might therefore be strongest in the subtropical belt, where cloudiness is low. However, the present simulations are insufficient to prove this hypotheses due to the large superimposed climate variability.

In order to analyze the seasonal response and the differences between the response over land- and sea-areas the correlation between the solar forcing response and the greenhouse warming pattern are computed using centered (r) and uncentered (r^*) correlations. While centered correlations focus on the similarity of patterns after the subtraction of the global mean warming pattern (which in these cases is common to all patterns), uncentered correlations take all pattern components into account. Correla-

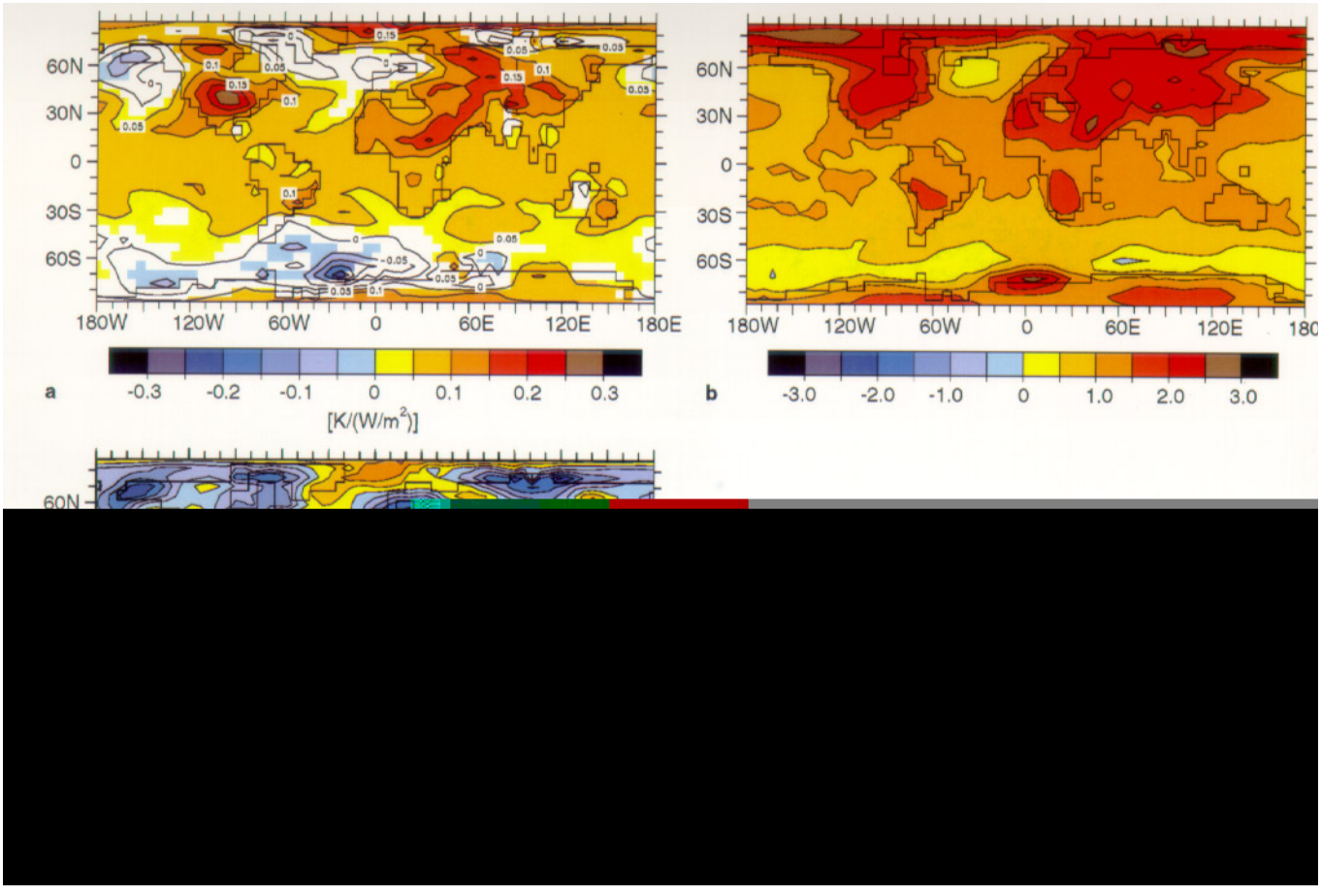

Fig. 3. a Horizontal response pattern (covariance normalized by variance of irradiance) of annually averaged near-surface temperature to changes in solar forcing (mean of both solar variability experiments) [K/(W/m^2)]. *White areas* indicate regions with a non-significant correlation (based on the 99% threshold of a t-test) between solar variability and surface temperature response. In these regions the contour lines have been drawn in to indicate the underlying pattern. **b** Shows for comparison the dominant climate change signal (first EOF) for greenhouse gas forcing (normalized). **c** Shows the difference between both patterns if these are normalized to the same variance

Table 1. Correlations disregarding the spatial mean (centered correlation *r*) and correlations including the spatial mean component (anomaly correlation *r**; see text) between the near-surface temperature response pattern of the solar forcing experiments and the first EOF of a greenhouse gas climate change experiment (Cubasch et al. 1996). Values in brackets indicate results if only areas are included which exhibit a significant correlation between the solar forcing time series and the temperature response

r	Annual	DJF	MAM	JJA	SON
Land and Sea	0.74 (0.79)	0.59 (0.75)	0.60 (0.75)	0.63 (0.70)	0.61 (0.75)
Land only	0.78 (0.78)	0.56 (0.70)	0.62 (0.73)	0.68 (0.64)	0.56 (0.66)
Sea only	0.62 (0.64)	0.55 (0.60)	0.51 (0.58)	0.49 (0.53)	0.55 (0.61)
*r**					
Land and Sea	0.88 (0.93)	0.80 (0.90)	0.79 (0.89)	0.79 (0.87)	0.84 (0.92)
Land only	0.92 (0.95)	0.81 (0.91)	0.81 (0.92)	0.84 (0.88)	0.87 (0.93)
Sea only	0.83 (0.91)	0.80 (0.89)	0.78 (0.87)	0.72 (0.83)	0.80 (0.90)

tions based only upon gridpoints where a significant correlation occurred between the solar forcing time series and the gridpoint temperature time series (see Fig. 3) are shown in parentheses in Table 1. The significance is estimated by the 99% threshold of a t-test. These correlations are based on a smaller area for seasonal than for annual mean values. Compared to correlations based on all data, the restricted correlations are higher with one exception (JJA-land case). This is caused by the higher uncertainty of the solar response and/or possible differences in the response in these areas. The correlations of the near surface temperature over oceans are systematically lower than

over land, which may be caused by longer response times of the oceanic mixed-layer compared to the land (see Sect. 3.3). The lowest correlations of all cases listed in Table 1 occurs for sea-areas in the season June, July, August (JJA).

This analysis suggests that the best chance to separate a solar signal from internal climate variability and greenhouse forcing should involve analysis of annual mean (smallest uncertainties for the solar response pattern) and JJA data over sea-areas (lowest correlation between solar and greenhouse response pattern). An attempt to do so is described in Sect. 3.5. It is based on an analysis of the observations in the phase space spanned by both patterns.

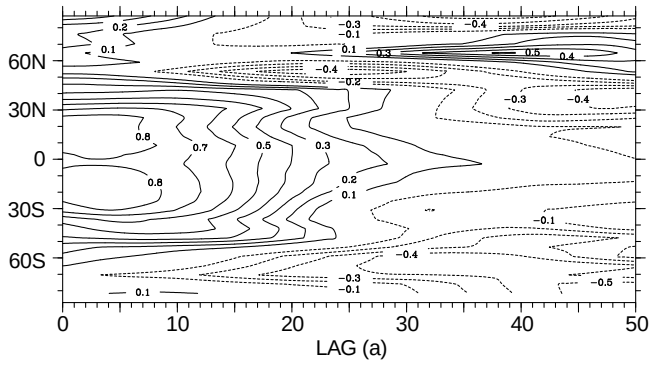

Fig. 4. Lag correlation between the solar forcing and zonally averaged near-surface temperature for sea-areas

3.3 Time-dependent response

The highest correlations for the near surface temperature occur in the tropical and subtropical regions. The largest amplitudes, on the other hand, can be observed in the extratropics (Fig. 3a; compare central North America). The highest correlations of more than 0.8 occur with a delay of three to five years. Figure 4 shows the zonal mean values of the correlation between surface temperature and solar variability for the sea-areas as a function of the time-lag. The region of the highest correlations is restricted to a latitude belt between 30 °N and 30 °S. Negative correlations of less than -0.4 can be observed in the northern mid latitudes with its maximum at a lag of approximately 25 y. This anticorrelation is followed by a positive correlation of 0.5 further to the north with a lag of approximately 40 y. This delayed response of the oceans can also be found in the thermohaline circulation. The maximum of the meridional stream function of the Atlantic, as a measure of the intensity of the meridional ocean circulation, is strongly anticorrelated (-0.8) with the solar forcing with a lag of 25–30 y. A high solar radiance leads to a weaker meridional circulation of the Atlantic accompanied by a negative anomaly of the near-surface temperature and vice versa. In particular the strong changes of the solar radiance between 1770 and 1830 (Fig. 1) strongly affect the thermohaline circulation. The decrease of more than 4 W/m^2 and the following increase of about 3 W/m^2 lead to changes of strength of the Atlantic meridional stream function more than 10% ($3 \cdot 10^6\ m^3/s$; not shown). Simulations of the climate response due to an enhancement of greenhouse gases show a similar response, i.e., a reduction of the North Atlantic thermohaline circulation (Manabe et al. 1991; Cubasch et al. 1992).

3.4 Vertical temperature response

In the troposphere, the vertical structure of the temperature response to solar variability (Fig. 5) resembles the one obtained by the greenhouse gas increase experiment, i.e., a general warming with a maximum in the upper tropical troposphere. In the stratosphere, the CO_2 experiment shows a general cooling which has also been found in the observations (Karoly et al. 1994; Santer et al. 1996; Tett et al. 1996), while in the solar variability experiments a small amount of warming is visible. However, the solar response in the stratosphere is characterized by high uncertainties indicated by the white areas in Fig. 5.

Solar variability induces a similar response in the stratosphere and surface (i.e., a synchronous warming or cooling) as found by Wetherald and Manabe (1975) and Hansen et al. (1984) in studies using uncoupled climate models and also as occurs in the internal variability of the GFDL model (Vinnikov et al. 1996). However, our stratospheric temperature response should be treated with caution because we did not include a varying UV component to the solar forcing. This effect and also anthropogenic ozone changes should influence the ozone content in the stratosphere and thus modify the stratospheric temperature response (Ramaswamy et al. 1996).

3.5 Relevance to greenhouse signal detection

Figure 1 showed that both solar forcing simulations predict a global mean temperature increase due to the hypothesized increase in solar radiation in this century, which is, as discussed already for 30- and 100-y global mean temperature trends, substantially smaller than the observed warming. For a more rigorous investigation into the cause of the twentieth century warming, we need to investigate if the significant warming which Hegerl et al. (1996, 1997) found in the recent observed 30-y trend patterns of near surface temperature between 1965 and 1994 might also be explained by solar forcing changes.

In order to determine whether the spatial pattern of the most recent observed temperature trends compares with the response patterns of solar and greenhouse gas induced climate change, the observed 30-y annual mean surface temperature trend patterns have been analyzed (trends fitted as described in Hegerl et al. 1996). We used annual mean and global data in regions with sufficient data coverage (i.e., gridpoints where after the middle of the twentieth century not more than a single year was missing between two years with data). Averaging over seasons and using all available spatial information should provide the best and least noise-contaminated data set for testing the solar response.

Since the dimension of the observed and simulated surface temperature trend pattern is as high as the number of gridpoints, a reduction in dimensions is required for

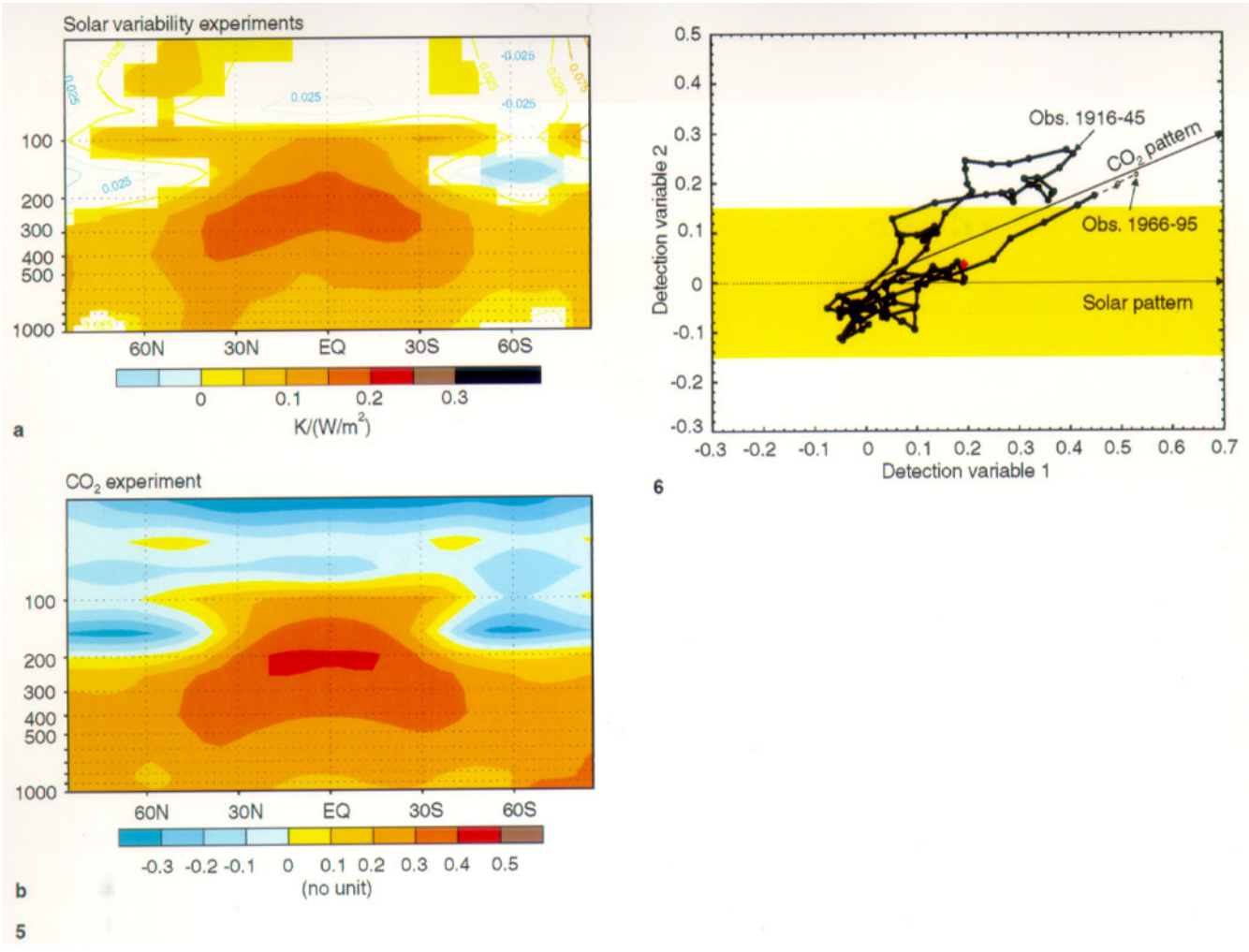

Fig. 5. a Response (covariance normalized by variance of radiance) of zonally averaged annual mean atmospheric temperature to changes in solar forcing (mean of both solar variability experiments) compared to **b** zonal mean of the first EOF of greenhouse-gas-induced climate change simulated with the same climate model (Hegerl et al. 1997). *White areas* indicate regions with a non-significant correlation between solar variability and the zonally averaged temperature response

Fig. 6. Relative importance of solar variability and greenhouse forcing with respect to trends in twentieth century observations (Jones and Briffa 1992). This figure compares the evolution of observed (1889–1995) annual mean 30-y near surface temperature trend patterns projected onto the solar pattern (*Solar Pattern*) and the greenhouse warming pattern (CO_2 *Pattern*). Detection variable 1 is related to the amplitude of the solar pattern, detection variable 2 to the amplitude of a second, independent pattern. Since response patterns to changes in solar forcing vary due to natural climate variability, the 95% confidence interval of solar response patterns (computed from the variability of detection variable 2) is shown as a *shaded band*. The *diamond* shows the last trend (1963–1992) of the mean of both solar forcing simulations, the *dashed line* the observed trends ending after the end of the solar simulation

a reasonable pattern comparison. We have done this by considering a plane which is embedded in the gridpoint space. This plane spans the solar response pattern and the greenhouse warming pattern and is, therefore, able to represent the difference between both patterns in an optimal way (see Hegerl et al. 1997 for full details). The anomaly correlations r^*, which are also shown in Table 1, represent the cosine of the angle between both patterns. Small differences in the correlations are caused by reduced data coverage in the observations.

Figure 6 shows the projection of the observed running 30-y trends in this two-dimensional phase space (the first trend is computed over the years 1860 to 1889 and the last trend over the years 1966 to 1995). The points in the phase space can be interpreted as the amplitude of the solar pattern (detection variable 1) and of a second independent pattern (detection variable 2) representing the difference between the greenhouse-gas forced and the solar forced climate change. This is formally the ortho-normalized greenhouse gas response pattern with respect to the solar pattern and is related (and similar, not shown) to the difference pattern shown in Fig. 3c. Patterns of 30-y observed trends, whose detection variables lie on the arrow "Solar Pattern" then agree (in the reduced space) with the pattern associated with solar forcing changes (Fig. 3a) and differ merely by the amplitude of the solar forcing pattern. Points on the arrow "CO2 Pattern" agree better with the greenhouse warming pattern.

The next step is to investigate if the recent 30-y trends are consistent with the solar forcing pattern. Due to the internal variability of climate alone, patterns associated with the response to solar forcing changes will not exactly agree with the solar pattern. In the phase space, this means that they will not project directly onto the arrow "Solar Pattern" but will spread around it. If a linear superposition of climate variability and solar forcing changes is assumed, the deviation of patterns from the solar forcing pattern, as associated with internal climate variability, can be estimated from the variations in detection variable 2 due to climate variability alone. Thus, the 95% confidence area for temperature patterns associated with changes in solar forcing plus climate variability can be estimated from the variations of detection variable 2 in 700 y of the control simulation (area shown by the yellow band in Fig. 6). If a different model control simulation is used for the estimate, for example the GFDL model (Stouffer et al. 1994) the results are very similar. If this estimate of the confidence interval is correct, then approximately 95% of the solar forcing trends in the model should lie in that confidence area. This has been confirmed by an analysis of the 30-y trend patterns occurring in the solar simulation (result not shown).

This exercise indicates that the most recent observed temperature trend patterns resemble more the greenhouse warming pattern (Fig. 6). The last observed trend pattern which can be compared to the solar simulation (1963–1992) lies marginally outside the confidence area for the solar simulation and thus cannot be explained by changes in solar variability alone. The latest observed trend (1966–1995) lies even further away and shows larger amplitude of warming. This further supports the conclusion that recent warming is not solar induced, since the number of sunspots was at a minimum at 1995 and thus a temperature decrease due to solar forcing should have been expected at that time. The latest trend in the solar forcing simulation (1963–1992), which is shown by a diamond in Fig. 6, lies well within the 95% confidence area. A separation between the modeled and observed value based only on the amplitude of the warming again yielded marginally significant disagreement between the solar simulation and the observations (at the 90% confidence level, if the ECHAM3/LSG variability was used to estimate internal climate variability). Such a separation is relatively difficult if based on only two simulations, since the simulated value is rather uncertain.

We have performed some sensitivity tests for this pattern separation, using summer data or restricting the analysis to ocean data. In most cases considered the observations agreed better with the greenhouse warming pattern. However, the results were not significant. These latter results may be due to a stronger influence of climate variability on seasonal data or by limiting the analysis to parts of the planet. For example, for the ocean data some areas of large pattern difference (e.g., the subtropical Pacific) do not have sufficient data coverage consistently since about 1950 and thus could not be included in the analysis. Trends ending before 1950 have been fitted by a least square fit to both patterns. In our view the limitations due to missing points introduce too much uncertainty to allow interpreting the strong agreement of the observed trends

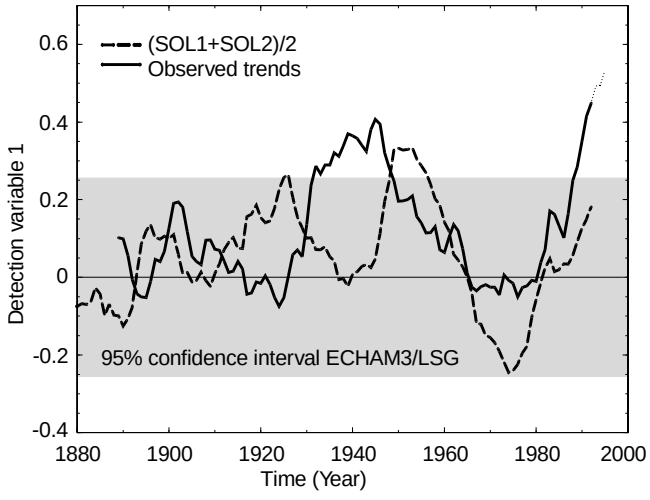

Fig. 7. Time evolution of the detection variable for the solar pattern (corresponding to detection variable 1 from Fig. 6) as computed from observed and model temperature trend patterns. The time axis denotes the final year of each 30-y trend pattern used to compute the detection variable. The latest observed trends cannot be compared to the simulations (*thin solid curve*). The simulated trend patterns have been computed from the average of both solar forcing simulations, without subtraction of the control simulation. The 95% confidence interval for the ECHAM3/LSG control simulation variability is shown by the *shaded area*

before 1950 (for example 1916–1945) with the greenhouse gas pattern (Fig. 6) as an indication that the warming in the early part of this century was greenhouse gas only induced. A more rigorous detection method that is able to take into account the uncertainty in the response associated with model noise has been used in Hegerl et al. (1997). The results of the latter work confirm our finding that it is improbable that solar forcing changes alone have caused the recent warming, however, also in this work the significance level of this finding was relatively low (90%).

Figure 7 shows the time evolution of detection variable 1 (i.e., of a regression of the observations upon the solar pattern only) compared to the detection variable using trend patterns from the average of both solar simulations instead of the observations. (The detection variable axis of this figure can be obtained by projecting Fig. 6 upon the horizontal axis). The model trend patterns are computed without subtracting the control simulation. Firstly, the control simulation does not exhibit much drift after the model year 1860. Secondly, subtracting the control simulation would induce additional noise which would make a comparison to the observed record problematic. Over large parts of the record both data seem rather uncorrelated. However, both time series exhibit strong events (significantly stronger than typical variations of the ECHAM3/LSG model control simulation, for which the 95% confidence interval is shown in the figure) for the trends ending in the middle of this century, with some difference in timing. This suggests a possible solar contribution to the mid-twentieth century warming. The timing offsets could reflect noise or uncertainties in forcing. For example, the calculations (Crowley and Kim 1996) with Lean et al.'s (1995) solar records indicate that the

twentieth century warming peaks about 20 y later with this index.

4 Summary and conclusion

A coupled ocean-atmosphere model has been forced with an generous estimate of solar variability since 1700 in order to assess its potential impact on climate. The coupled model mainly responds to variations of solar irradiance in near-surface temperature with a time lag of less than 10 y over most regions of the globe. However, there is a 25–30 y delayed response over sea-areas, particularly the North Atlantic, which is also visible in its thermohaline circulation. The dominant response in the model is at the centennial-scale Gleissberg cycle, with peak-to-trough changes in global temperature of the order of 0.5 K and with a stronger response to a decrease of the solar intensity than to an increase.

The prime response to an increase of solar irradiance is an increase in the land–sea contrast, similar to the effect of an enhancement of greenhouse gases. However, differences between both patterns exist which are strongest in summer over parts of the subtropical ocean. The significance of these differences and the possible physical mechanism responsible for it cannot yet be determined due to the restricted sample size.

Although the vertical structure of the warming between greenhouse gas and solar warming is similar in the troposphere, differences occur in the stratosphere. The greenhouse gas response pattern generally shows a cooling in the stratosphere, while an increase in solar radiation tends to increase temperatures there, confirming the equilibrium results obtained by Wetherald and Manabe (1975) and Hansen et al. (1984). The sustained observed stratospheric cooling since the late 1950s (Tett et al. 1996) cannot be explained by solar variability. Other effects, such as ozone variations, also have to be considered in this layer of the atmosphere.

Over the last 30 y, the modeled global warming due to the solar radiance increase explains about 40% of the observed global warming. The global mean temperature trends over 30 and 100 years in the solar variability simulations are significantly smaller than in the observations. The warming pattern of the recently observed 30-y trends does not seem consistent with a response to solar variability alone and points towards the CO_2 pattern. Uncertainties in this finding are caused by our limited knowledge of climate variability, uncertainties in the solar forcing, and uncertainties in the response as estimated by only two simulations. It should be mentioned in this context that the agreement between the observations and the aerosol response pattern is even better than that with greenhouse gases alone (Santer et al. 1995; Hegerl et al. 1997).

These results suggest that, if the solar irradiance estimates are valid, the changes induced by solar variability could have contributed significantly to the climate changes on multi-decadal time scales. A substantial amount of variability on multi-decadal time scale may therefore be forced. These results may explain some of the large differences in variance between paleo-data (Bradley and Jones 1993) and estimates of unforced variability from control runs of coupled models (Barnett et al. 1996). It should also be noted that there is also evidence for decadal scale variations in volcanism (Robock 1979; Crowley et al. 1997) that would further increase climate variability on this time scale. For example, compositing Southern Hemisphere ice core records of volcanism from 1600 to the present indicate that as many as nine volcanic eruptions (some very large) occurred in the 33 y interval from 1803–1835 (Crowley et al. 1997). Modeling studies suggest that this pulse of volcanism may have lowered global temperatures by several tenths of a degree for 30 y (T.J. Crowley and K.-Y. Kim in preparation).

We conclude that, even if the multi-decadal estimates of solar variability are valid, our results suggest that solar forcing changes may contribute to the temperature record of the twentieth century warming but cannot explain it alone. Our attempts to distinguish between solar forced and anthropogenic climate change are, however, subject to many uncertainties (limited knowledge of the solar response pattern, highly uncertain knowledge of the solar forcing history, uncertainties in our knowledge of climate variability, and lack of observational data in critical areas). More simulations, more reliable solar forcing time series and a full time-space analysis of the observed temperature record are required to conclude with confidence that solar forcing changes alone are inconsistent with the observed temperature record. The response pattern to an anthropogenic increase in sulfate aerosols has also not yet been included, since we wanted to assess first if the greenhouse forcing or the solar forcing could be responsible for the recent warming. Including the latter pattern should increase the similarity between modeled and observed temperature patterns (Santer et al. 1995; Hegerl et al. 1997) even further.

Experiments with coupled climate models provide a wealth of additional information which we will report on in future studies. Future investigations of such effects may better enhance our understanding of climate change in the twentieth century and the potential effect of solar variability on the instrumental and paleo-climatic record.

Acknowledgements. The authors thank K. Hasselmann, E. Roeckner and C. Covey for their scientific support, P.D. Jones for the surface temperature data and D. Hoyt for the solar time series. The research has been supported by the German Ministry for Education, Research and Technology (BMBF), the Max-Planck-Gesellschaft, the EC Environmental program (EV5V-CT92-0123, ENV4-CT95-0102), the National Science Foundation grant ATM-9529109 (TJC) and NOAA's Office of Global Program's Climate Change Data and Detection Program Element (GCH). The authors are grateful to the staff of the DKRZ for their technical support.

References

Barnett TP, Santer BD, Jones PD, Bradley R, Briffa KR (1996) Estimates of low frequency natural variability in near-surface temperature. The Holocene 6 : 255–263

Bradley RS, Jones PD (1993) 'Little Ice Age' summer temperature variations: their nature and relevance to recent global warming trends. The Holocene 3 : 367–376

Covey C, Santer BD, Cohen-Solal E (1996) CMIP: a study of climate models and natural climate variability. In: Kinter III, J L, Schneider EK (eds) Proc Workshop on Dynamics and Statistics of Secular Climate Variations, Miramare-Trieste, Italy, 4–8 December 1995, Rep 26, Center for Ocean–Land–Atmosphere Studies, 11–15

Crowley TJ, Kim K-Y (1993) Towards development of a strategy for determining the origin of decadal-centennial scale climate variability. Quat Sci Rev 12: 375–385

Crowley TJ, Kim K-Y (1996) Comparison of proxy records of climate change and solar forcing. Geophys Res Lett 23: 359–362

Crowley TJ, Quinn TM, Taylor FW, Henin C, Joannot P (1997) Evidence for a volcanic cooling signal in a 335 year coral record from New Caledonia. Paleoceanogr (in press)

Cubasch U, Hasselmann K, Höck H, Maier-Reimer E, Mikolajewicz U, Santer BD, Sausen R (1992) Time-dependent greenhouse warming computations with a coupled ocean-atmosphere model. Clim Dyn 8: 55–69

Cubasch U, Santer BD, Hellbach A, Hegerl G, Höck H, Maier-Reimer E, Mikola-jewicz U, Stössel A, Voss R (1994) Monte Carlo climate change forecasts with a global coupled ocean-atmosphere model. Clim Dyn 10: 1–19

Cubasch U, Hegerl G, Hellbach A, Höck H, Mikolajewicz U, Santer BD, Voss R (1995) A climate change simulation starting 1935. Clim Dyn 11: 71–84

Cubasch U, Hegerl G, Waszkewitz J (1996) Prediction, detection and regional assessment of anthropogenic climate change. Geophysica 32: 77–96

DKRZ (1993) The ECHAM3 atmospheric general circulation model. Tech Rep 6, DKRZ, Bundesstr 55, Hamburg, Germany

Friis-Christensen E, Lassen K (1991) Length of the solar cycle: an indicator of solar activity closely associated with climate. Science 254: 698–700

Hansen JE, Lacis A, Rind D, Russell G, 1984: Climate sensitivity: analysis of feedback mechanisms. In: Hansen JE, Takahsi T (eds) Climate processes and climate sensitivity, Maurice Ewing Series 5, AGU, pp 130–163

Hasselmann K, Bengtsson L, Cubasch U, Hegerl GC, Rohde H, Roeckner E, von Storch H, Voss R, Waszkewitz J (1996) Detection of anthropogenic climate change using a fingerprint method. MPI Rep 168, MPI für Meteorologie, Hamburg, FRG

Hegerl GC, von Storch H, Hasselmann K, Santer BD, Cubasch U, Jones PD (1996) Detecting greenhouse gas induced climate change with an optimal fingerprint method. J Clim 9: 2281–2306

Hegerl GC, Hasselmann K, Cubasch U, Mitchell JBF, Roeckner E, Voss R, Waszkewitz J (1997) On multi-fingerprint detection and attribution of greenhouse gas- and aerosol forced climate change. Clim Dyn (accepted)

Hoyt DV, Schatten KH (1993) A discussion of plausible solar irradiance variations, 1700–1992. J Geophys Res 98: 18 895–18 906

IPCC (1990) Climate change: the IPCC scientific assessment. Houghton J, Jenkins GJ, Ephraums JJ (eds), Cambridge University Press, 364 pp

IPCC (1996) Climate change 1995: the science of climate change. Houghton JT, Meira Filho LG, Callander BA, Harris N, Kattenberg A, Maskell K (eds), Cambridge University Press, Cambridge, 572 pp

Jones PD, Briffa KR (1992) Global surface air temperature variations during the twentieth century: part 1, spatial, temporal and seasonal details. The Holocene 2: 165–179

Karoly DJ, Cohen JA, Meehl GA, Mitchell JFB, Oort AH, Stouffer RJ, Wetherald RT (1994) An example of fingerprint detection of greenhouse climate change. Clim Dyn 10: 97–105

Kiehl JT, Briegleb BP (1993) The relative role of sulfate aerosols and greenhouse gases in climate forcing. Science 260: 311–314

Lean J (1997) The Sun's variable radiation and its relevance to Earth. Annu Rev Atron Astrophys 35: 33–67

Lean J, Beer J, Bradley R (1995) Reconstruction of solar irradiance since 1610: implications for climate change. Geophys Res Lett 22: 3195–3198

Maier-Reimer E, Mikolajewicz U, Hasselmann K (1993) Mean circulation of the Hamburg LSG OGCM and its sensitivity to the thermohaline surface forcing. J. Phys Oceanogr 23: 731–757

Manabe S, Stouffer RJ, Spelmann MJ, Bryan K (1991) Transient responses of a coupled ocean-atmosphere model to gradual changes of atmospheric CO_2: I Annual mean response. J Clim 4: 785–818

Mitchell JM, Stockton CW, Meko DM (1979) Evidence for a 22-year rhythm of drought in the western United States related to the Hale solar cycle since the 17th century. In: McCormac BM, Seliga TA (eds) Solar-terrestrial influences on weather and climate. Reidel, Hingham, Massachusetts, pp. 125–144

North GR (1984) Empirical orthogonal functions and normal models. J Atmos Sci 41: 879–887

Preisendorfer RW (1988) Principal component analysis in meteorology and oceanography. Developments in Atmospheric Sciences 17, Elsevier

Ramaswamy V, Schwarzkopf MD, Randel WJ (1996) Fingerprint of ozone depletion in the spatial and temporal pattern of recent lower-stratospheric cooling. Nature 382: 616–618

Reid GC (1991) Solar irradiance variations and the global sea surface temperature record. J Geophys Res 96: 2835–2844

Rind D, Overpeck J (1993) Hypothesized causes of decade-to-century scale climate variability: climate model results. Quat Sci Rev 12: 357–374

Robock A (1979) The "Little Ice Age": Northern Hemisphere average observations and model calculations. Science 206: 1402–1404

Roeckner E, Arpe K, Bengtsson L, Brinkop S, Dümenil L, Esch M, Kirk E, Lunkeit F, Ponater M, Rockel B, Sausen R, Schlese U, Schubert S, Windelband M (1992) Simulation of the present-day climate with the ECHAM model: Impact of model physics and resolution. Rep 93, Max-Planck-Institut für Meteorologie, Bundesstr 55, Hamburg, Germany

Roeckner E, Siebert T, Feichter J (1995) Climatic response to anthropogenic sulfate forcing simulated with a general circulation model. In: Charlson RJ, Heintzenberg J (eds) Aerosol forcing of climate. J Wiley and Sons

Santer BD, Brüggemann W, Cubasch U, Hasselmann K, Höck H, Maier-Reimer E, Mikolajewicz U (1994) Signal-to-noise analysis of time-dependent greenhouse warming experiments. Part 1: pattern analysis. Clim Dyn 9: 267–285

Santer BD, Taylor KE, Wigley TML, Penner JE, Jones PD, Cubasch U (1995) Towards the detection and attribution of an anthropogenic effect on climate. Clim Dyn 12: 77–100

Santer BD, Taylor KE, Wigley TML, Jones PD, Karoly DJ, Mitchell JFB, Oort AH, Penner JE, Ramaswamy V, Schwarzkopf MD, Stouffer RJ, Tett S (1996a) A search for human influences on the thermal structure of the atmosphere. Nature 382: 39–46

Santer BD, Wigley TML, Barnett TP, Anyamba E (1996b) Detection of climate change, and attribution of causes. In: Houghton JT, Meira Filho LG, Callander BA, Harris N, Kattenberg A, Maskell K (eds) Climate change, 1995: the science of climate change. Cambridge University Press, Cambridge, pp. 407–443

Spelman MJ, Manabe S (1984) Influence of oceanic heat transport upon the sensitivity of a model climate. J Geophys Res 89: 571–586

Stouffer RJ, Manabe S, Vinnikov KY (1994) Model assessment of the role of natural variability in recent global warming. Nature 367: 634–636

von Storch J, Kharin V, Cubasch U, Hegerl GC, Schriever D, von Storch H, Zorita E (1996) A 1260-year control integration with the coupled ECHAM1/LSG general circulation model. Max-Planck-Institut für Meteorologie, Report 198

Tett SFB, Mitchell JFB, Parker DE, Allen MR (1996) Human influence on the atmospheric vertical temperature structure: detection and observations. Science 247: 1170–1173

Vinnikov KY, Robock A, Stouffer RJ, Manabe S (1996) Vertical patterns of free and forced climate variations. Geophys Res Lett 23: 1801–1804

Voss R, Sausen R, Cubasch U (1996) A multiple-century climate change simulation with a periodically synchronously coupled atmosphere-ocean general circulation model. WMO/TD 734, WMO, Geneva, 926–927

Voss R, Sausen R, Cubasch U (1997) Periodically synchronously coupled integrations with the atmosphere-ocean general circulation model ECHAM3/LSG. Rep 229, Max-Planck-Institut Für Meteorologie, Bundesstr. 55, Hamburg, Germany

Wetherald RT, Manabe S (1975) The effects of changing the solar constant on the climate of a general circulation model. J Atmos Sci 32: 2044–2059

Wigley TML, Kelly PM (1990) Holocene climate change, ^{14}C wiggles and verification in solar irradiance. Philos Trans R Soc (London) A330: 547–560

Wigley TML, Raper, SCB (1990) Climatic change due to solar irradiance changes. Geophys Res Lett 17: 2169–2172